Degradation of Acid Orange 7 by peroxymonosulfate activated by cupric oxide

Guo Li, Zhihui Zhong, Chun Yang, Qiang He and Guilong Peng

ABSTRACT

Copper oxide (CuO) was prepared through a facile one-step hydrothermal method and used as an activator of peroxymonosulfate (PMS) for the degradation of azo dye Acid Orange 7 (AO7), as a model organic pollutant. The effects of several parameters on the decolorization efficiency on AO7 were investigated. The degradation kinetic characteristics were studied by investigating the effect of different operational parameters including CuO dosage, pH and initial AO7 concentration. The reactive radical species were determined indirectly by way of radical quenching tests, as well as directly by *in situ* electron paramagnetic resonance technique spin trapping tests. In a 15 min reaction using 5 mM PMS, a CuO dosage of 0.1 g/L, at pH 6.65, 95.38% of 40 mg/L AO7 can be removed. This study provides an effective oxidative system for AO7 removal by CuO/PMS heterogeneous process at ambient temperature.

Key words | Acid Orange 7, CuO, degradation, peroxymonosulfate, PMS

Guo Li
Chun Yang (corresponding author)
Qiang He
Guilong Peng
Key Laboratory of Eco-Environment of Three Gorges Region of Ministry of Education,
Chongqing University,
Chongqing 400045,
China
E-mail: *c.yang@cqu.edu.cn*

Zhihui Zhong
Department of Orthopaedics,
Fuzhou Second Hospital Affiliated to Xiamen University,
Fuzhou 350007,
China

Guilong Peng
School of Environment, Beijing Key Laboratory for Emerging Organic Contaminants Control, State Key Joint Laboratory of Environment Simulation and Pollution Control (SKLESPC),
Tsinghua University,
Beijing 100084,
China

INTRODUCTION

Sulfate radical-based ($SO_4^{\bullet-}$) advanced oxidation processes (SR-AOPs) have received a great deal of attention in recent years for removing environmental organic contaminants, such as phenol, dyes, perfluorinated compounds and pharmaceuticals (Ahmad *et al.* 2013; Duan *et al.* 2015; Oh *et al.* 2016). $SO_4^{\bullet-}$ can be generated from peroxymonosulfate (PMS) and peroxodisulfate (PDS) by UV, heat, base or transition metals (Guan *et al.* 2013; Qi *et al.* 2015). Compared with PDS, PMS is easier to activate by transition metals due to the asymmetric molecular structure (Anipsitakis & Dionysiou 2004). Homogeneous catalytic oxidation by PMS coupled with transition metals showed efficient decontamination of organic pollutants. Among the tested transition metals including Ag(I), Ce(III), Co(II), Fe(II), Fe(III), Mn(II), Ni(II), Ru(III) and V(III), Co(II) is the most effective catalyst of PMS activation for the production of sulfate radicals (Ding *et al.* 2013; Hu & Long 2016). However, cobalt has been recognized as a possible human carcinogen by the International Agency for Research on Cancer (IARC). Thus, using cobalt as a catalyst has limitations in practical applications. Consequently, the development of efficient catalysts for PMS activation remains a priority.

Copper-based catalysts have been intensively studied in recent years, and copper is not regarded as a potential carcinogen. In particular, CuO has been used with peroxymonosulfate (PMS) and peroxydisulfate (PDS) for the degradation of organic contaminants (Liang *et al.* 2013; Zhang *et al.* 2014; Du *et al.* 2017; Hu *et al.* 2017; Li *et al.* 2017b; Luo *et al.* 2018). The preparation methods for CuO in these studies used $Cu(NO_3)_2.3H_2O$ calcined in a closed muffle under high temperature (300–450 °C) or prepared by a hydrothermal method under high temperature (180–200 °C) and high pressure. However, high calcination temperature and the complicated preparation methods may hamper wider application. The size of the

doi: 10.2166/aqua.2018.096

hydrothermal reactors (Teflon-lined autoclave) and the requirement of high pressure significantly limit preparation on a large scale. So, it is of great interest to study an economical and efficient method of preparing CuO and its use in the activation of persulfates for organic pollutant degradation.

Azo dyes have the -$N=$N- chromophoric group and may be monoazo, diazo or polyazo dyes, and are widely used by the textile industries, accounting for over 50% of all commercial dyes (López-López *et al.* 2007; Li *et al.* 2017a). These dyes are difficult to degrade by biological treatment methods due to their complex structure and their stability (Brillas & Martínez-Huitle 2015; Li *et al.* 2015). Therefore, in this study, we report a facile and low-cost method for the preparation of CuO. Acid Orange 7 (AO7), a typical azo dye and commonly used as a model compound for the study of dye degradation, and the effects of various reaction parameters such as initial PMS and AO7 concentrations, CuO dosage and solution pH are investigated. Furthermore, the electron paramagnetic resonance technique (EPR) and radical scavenging experiments using ethanol (EtOH), tert-butanol (TBA) and AO7 have been performed to investigate the radicals generated in the reaction system.

EXPERIMENTAL

Chemicals and materials

PMS ($2KHSO_5{\cdot}KHSO_4{\cdot}K_2SO_4$ as Oxone) and 5,5-dimethyl-1-pyrrolidine N-oxide (DMPO), were purchased from Sigma-Aldrich (St. Louis, MO, USA). Cupric nitrate ($Cu(NO_3)_2{\cdot}3H_2O$), ammonia ($NH_3.H_2O$), sodium hydroxide (NaOH), sulfuric acid (H_2SO_4), ethanol (EtOH), tert-butyl alcohol (TBA) and other chemical agents were purchased from Sinopharm Chemical Reagent Co., Ltd, (Shanghai, China). All chemicals were at least analytical grade and were used as received without further purification. A basic FE28 pH meter (Mettler Toledo, Shanghai, China) was used to measure the pH values. Ultrapure water (18.2 MΩ·cm) from a Milli-Q academic water purification system was used to prepare all the solutions required in the present work.

Preparation of CuO and characterization

CuO catalyst was fabricated using a modified simple and one-step hydrothermal method according to the previously reported method (Lei *et al.* 2015). Typically, 4.8 g $Cu(NO_3)_2{\cdot}3H_2O$ was dissolved in ultrapure water (40 mL) to obtain a mixture solution and transferred into a 50 mL glass conical flask, followed by the addition of $NH_3.H_2O$. The mixture was stirred vigorously and heated in a water bath at 80 °C for 6 h, and aerated throughout the heating process. After being cooled to room temperature, the mixture was then centrifuged, and the desired solids were collected and dried at 105 °C. The surface morphology was characterized on an SU-8010 microscope (Hitachi, Japan). The crystal structure was characterized by X-ray diffraction (XRD, Rigaku S2, Japan).

Catalytic degradation experiment

The degradation experiments were carried out in a 250 mL conical flask at 25 °C. Desired amount of PMS and AO7 stock solutions were added to solution to a final volume of 200 mL. Solution pH was adjusted by H_2SO_4 or NaOH. Then the reaction was initiated once the catalyst was added. During reaction processes, the solution was stirred with a magnetic stirrer to ensure a complete mixing state. At the given reaction time intervals, approximately 1 mL of sample was withdrawn and the AO7 content was determined immediately (within 30 s).

Analytical methods

The concentration of the AO7 solution was measured immediately at wavelengths of 484 nm using a DR5000 UV-vis spectrophotometer (HACH, Loveland, CO, USA). The decolorization efficiency of AO7 and rate constant values were calculated according to Equations (1) and (2), respectively:

$$\text{Decolorization } (\%) = 100 \times (C_0 - C_t)/C_0 \quad (1)$$

$$\ln (C_t/C_0) = -k_{obs}t \quad (2)$$

where C_0 is the initial AO7 concentration, C_t is the AO7 concentration at time t in the CuO/PMS system, and k_{obs}

is the pseudo-first-order constant (min^{-1}). Total organic carbon (TOC) analysis was performed using a TOC analyzer (TOC-L CPN, Shimadzu, Kyoto, Japan). Specific oxidant efficiency (SOE) was calculated based on Equation (3) according to the literature reported by Jaafarzadeh *et al.* (2017).

$$SOE = (TOC_0 - TCO_t)/(Oxidant_0 - Oxidant_t) \quad (3)$$

where the unit of TOC and oxidant are expressed based on mg/L. SOE value presents removed TOC per reacted oxidant, the higher SOE represents the higher efficiency of oxidant consumption. The concentration of PMS was measured based on iodometric titration procedure (Lee *et al.* 2015).

RESULTS AND DISCUSSION

Catalyst characterization

Figure 1 shows the representative scanning electron microscopy (SEM) images of CuO particles. The SEM observation indicated that CuO was composed of fine particles with grain sizes of 2–5 μm. Each microsphere is composed of small nanoleaflets with one end growing together to form a center and another end radiating laterally from this center. The XRD pattern is shown in Figure 2. The peaks of the sample match well with JCPDS card no. 01-089-2530 (Rao *et al.* 2018). All the diffraction peaks could be readily indexed to the monoclinic CuO. The result also showed a highly crystalline and single-phase structure of CuO.

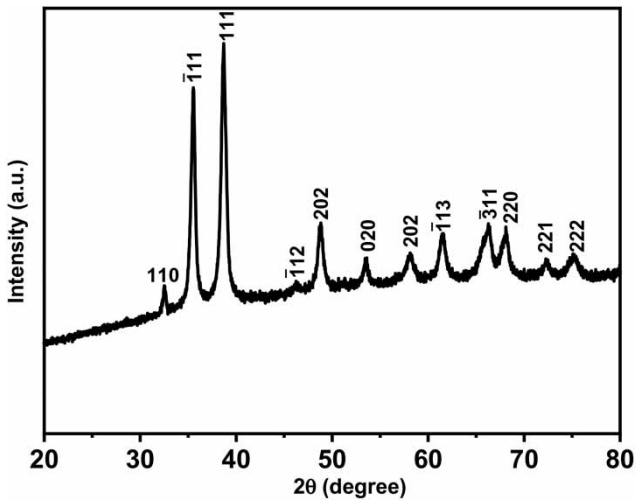

Figure 2 | The XRD patterns of the prepared CuO catalyst.

Catalytic oxidation of AO7

The reactivity of CuO as PMS catalyst was studied by the reaction of degradation of AO7. As a comparison, experiments were carried out in different systems (Figure 3). It can be clearly seen that only 2.69% and 3.38% of AO7 was decolorized within 15 min reaction time in the control systems with only either PMS and Cu^{2+}, respectively (with a total Cu amount the same as that in the used CuO). On the contrary, nearly 95% of AO7 was decolorized within 15 min in the CuO/PMS system. Obviously, CuO as a catalyst significantly enhanced the decolorization efficiency of the AO7.

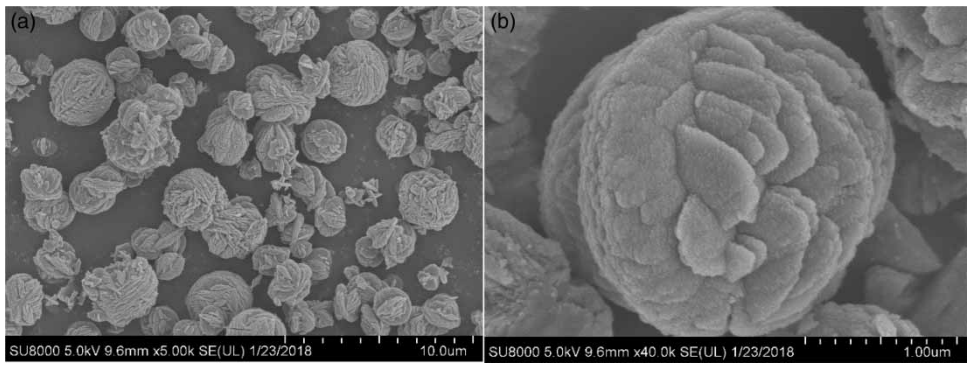

Figure 1 | SEM images of the prepared CuO catalyst at (a) 10 μm and (b) 1 μm scales.

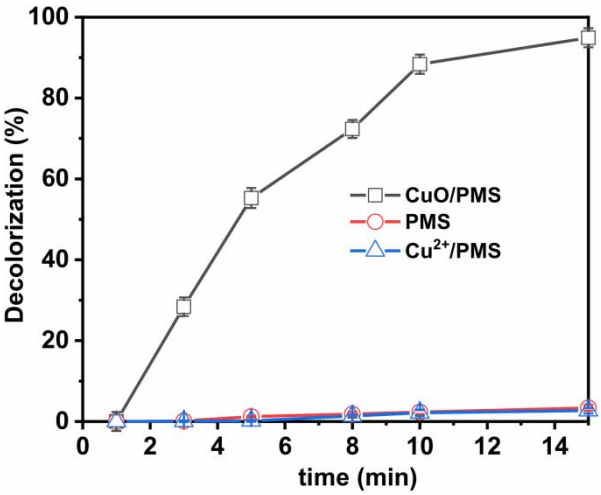

Figure 3 | The degradation of AO7 versus time in different systems. Conditions: [AO7] = 40 mg/L; [PMS] = 5 mM; [CuO] = 0.1 g/L; room temperature.

Effect of catalyst dosage

The influence of catalyst amount on the AO7 degradation was studied by varying the concentration of catalysts from 0.05 to 0.20 g/L. At the given dosage of PMS (5 mM), the decolorization efficiency increased remarkably with increasing of the catalyst dosage (Figure 4), and the values of k_{obs} increased from 0.00398 to 0.5210 min^{-1} when CuO concentration was raised from 0.05 to 0.2 g/L. This was because the increasing amount of catalyst could increase the number of active sites, which is beneficial to the formation of more reactive radicals. For example, at 0.05 g/L CuO, only 21.89% AO7 decolorization efficiency occurred in 5 min; however, when the concentration of CuO was 0.2 g/L, the decolorization efficiency could reach 96.12%, an enhancement of AO7 removal rate of over four times.

Effect of concentration of PMS

PMS dosage is the main factor affecting the production of sulfate and hydroxyl radicals, that is, PMS is the main source of sulfate and hydroxyl radicals. As depicted in Figure 5, the values of k_{obs} were 0.935, 0.2111, 0.1715 and 0.0587 min^{-1} for the concentration of PMS of 2, 5, 10 and 20 mM, respectively. The AO7 decolorization efficiency increased from 84.29 to 94.91% when the concentration of PMS increased from 2.0 mM to 5.0 mM. However, when the PMS concentration increased to 20.00 mM, the decolorization efficiency decreased to 58.61%. This might be attributed to the unfavorable consumption of generated reactive oxygen species by the excess PMS. Although increasing the amount of PMS is helpful for increasing the production of reactive radicals, higher PMS concentration has a negative effect on the concentration of sulfate and hydroxyl radicals. Excessive PMS can scavenge both sulfate and hydroxyl radicals and decrease the removal efficiency (see Equations (4) and (5) (Barzegar *et al.* 2018). $SO_5^{\bullet-}$ is the main product of these reactions, which is a weaker oxidant

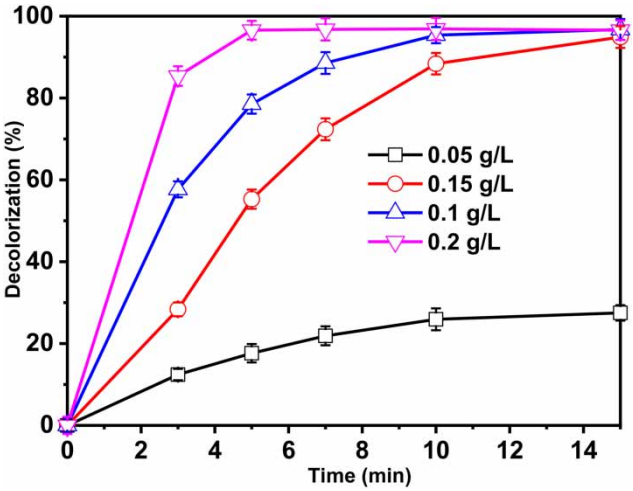

Figure 4 | Effect of catalyst concentration on the decolorization efficiency of AO7. Conditions: [AO7] = 40 mg/L; [PMS] = 5 mM; [CuO] = 0.1 g/L; room temperature.

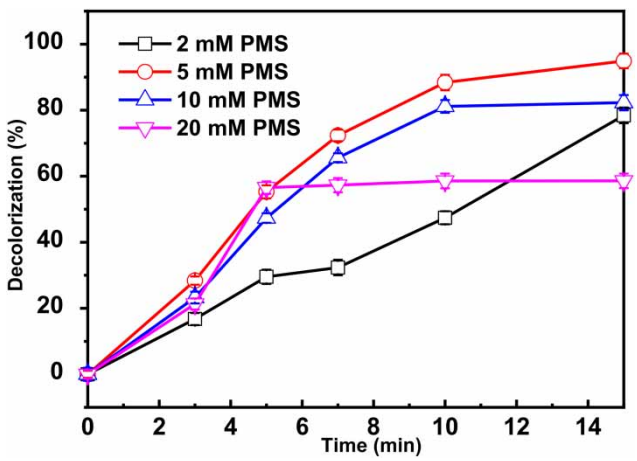

Figure 5 | Effect of PMS concentration on the decolorization efficiency of AO7. Conditions: [AO7] = 40 mg/L; [CuO] = 0.1 g/L; room temperature.

with redox potential of 1.1 V (Ahmadi & Ghanbari 2018).

$$HSO_5^- + SO_4^{\bullet -} \rightarrow SO_4^{2-} + SO_5^{\bullet -} + H^+ \quad (4)$$

$$HSO_5^- + \bullet OH \rightarrow SO_5^{\bullet -} + H_2O \quad (5)$$

Effect of initial AO7 concentration

The effect of the initial concentration of AO7 was investigated under different initial concentrations of AO7 (20, 30, 40 and 50 mg/L) and the results are shown in Figure 6. It can be observed that AO7 decolorization efficiency decreased with increasing initial AO7 concentrations. The rate constant values (k_{obs}) for AO7 decolorization at initial AO7 concentrations of 20–50 mg/L were from 0.3088 to 0.1766 min^{-1}. For the whole range of initial concentrations, AO7 decolorization efficiencies of 90.39–95.38.0% were achieved within 15 min, which indicates that the CuO/PMS system has excellent AO7 decolorization performance at various concentration levels. When initial AO7 concentration is low, radical production will be higher than the consumption rate leading to a higher decolorization efficiency, while more reaction time for complete decolorization of AO7 is required at higher concentrations of AO7.

Effect of pH

The decolorization of AO7 was investigated at different initial pH values and the results are presented in Figure 7.

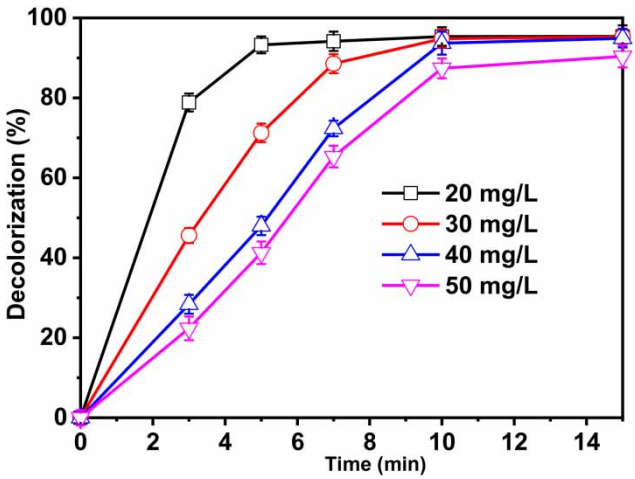

Figure 6 | AO7 decolorization under different initial concentration of AO7. Conditions: [PMS] = 5 mM; [CuO] = 0.1 g/L; room temperature.

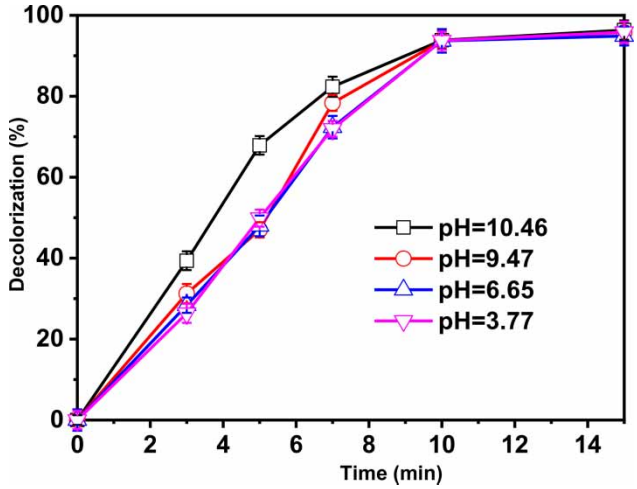

Figure 7 | Effect of pH on the decolorization efficiency of AO7. Conditions: [AO7] = 40 mg/L; [CuO] = 0.1 g/L; [PMS] = 5 mM; room temperature.

Results revealed that increasing pH led to an increase in decolorization efficiency. PMS and AO7 had pK_a values of 9.4 and 11.4, respectively (Ball & Edwards 1956; Bandara *et al.* 1999). PMS mainly existed as HSO_5^- in the solution at acidic and neutral pH values, and a small fraction of PMS existed as SO_5^{2-} at pH below 9.4 (Zhang *et al.* 2013). Meanwhile, PMS existed mostly in the form of SO_5^{2-} at pH range of 9.5–10.5, and SO_5^{2-} was easier to activate than HSO_5^- in heterogeneous catalytic oxidation (Guan *et al.* 2013). AO7 mainly existed in the form of mono-anion ($AO7^-$) and further dissociated into the dianion form ($AO7^{2-}$) at pH > 11.4. Overall, in this system, it is more favorable for the decolorization of AO7 under base condition (pH > 9). This result was consistent with previous reports that AO7 can be efficiently decolorized in a base/PMS system (Deng *et al.* 2017).

Effect of HCO_3^-

It is well known that bicarbonate can not only serve as a radical scavenger for •OH and $SO_4^{\bullet -}$ (Equations (4) and (5)) (Deng *et al.* 2013a, 2013b), but can also strongly influence solution pH. It was observed that decolorization rate increased with increasing HCO_3^- concentration from 0 to 10 mM (Figure 8), a phenomenon which may be attributed to three reasons. First, PMS can also be activated at high HCO_3^- concentrations. Yang *et al.* (2010) reported that

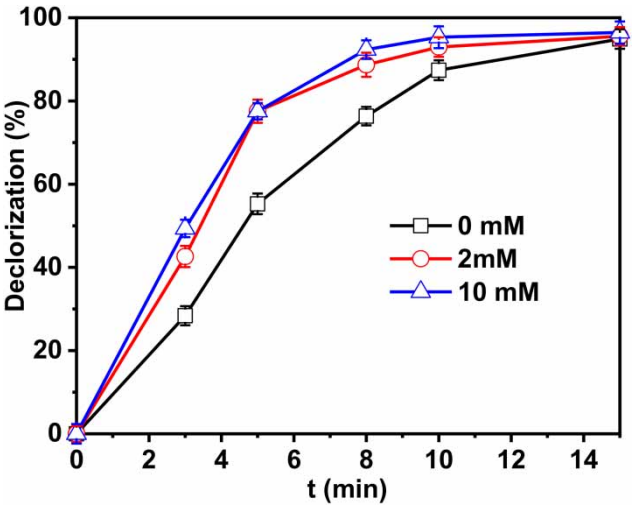

Figure 8 | Effect of HCO_3^- on the decolorization efficiency of AO7. Conditions: [AO7] = 40 mg/L; [CuO] = 0.1 g/L; [PMS] = 5 mM; room temperature.

AO7 can be efficiently decolorized in HCO_3^-/PMS system and inferred that the generation of $SO_4^{\bullet-}$ played the decisive role. Second, due to the buffering ability of $NaHCO_3$, pH remained in the 8.11–9.96 range during the reaction process, AO7 can be efficiently decolorized in base/PMS system, and singlet oxygen ($^1O_2$) and superoxide anion radical ($O_2^{\bullet-}$) were the dominant reactive oxygen species in AO7 decolorization (Deng *et al.* 2017). Third, carbonate radical ($CO_3^{\bullet-}$) is a selective one-electron oxidant ($E_0 = 1.78$ V at pH 7) and has varied reactivity towards organic compounds (Neta *et al.* 1988; Liu *et al.* 2016).

Reactive species and possible mechanism

To identify the radical species generated in the CuO/PMS process, radical quenching tests were performed using TBA and EtOH, respectively. Hydroxyl radical reaction can be scavenged by TBA (k_{TBA}, $\bullet OH = (3.8–7.6) \times 10^8\ M^{-1}\ s^{-1}$), while the sulfate radical reacts with TBA much more slowly (k_{TBA}, $SO_4^{\bullet-} = (4.0–9.1) \times 10^5\ M^{-1}\ s^{-1}$) (Neta *et al.* 1988). EtOH can be used to capture •OH and $SO_4^{\bullet-}$(k_{EtOH}, $\bullet OH = (1.8–2.8) \times 10^9\ M^{-1}\ s^{-1}$; k_{EtOH}, $SO_4^{\bullet-} = (1.6–7.7) \times 10^7\ M^{-1}\ s^{-}$) (Jiang *et al.* 2015). As depicted in Figure 9(a), the presence of 1 M TBA significantly suppressed the oxidation process, with the decolorization efficiency decreasing from 95.38% to 68.61%, indicating that •OH were produced in the CuO/PMS system. For the EtOH-added test, the presence of 1 M EtOH significantly suppressed the oxidation process, with the decolorization efficiency decreasing from 95.38% to 32.52%. One possible reason could be if a greater amount of •OH existed in the system accompanied with negligible $SO_4^{\bullet-}$, EtOH reacts faster with •OH than TBA, thus leading to more •OH being scavenged in the EtOH-added system than the TBA-added system. Consequently, a stronger inhibition effect on the decolorization efficiency could be observed in the EtOH-added system.

To further distinguish the reactive radical species in the CuO/PMS system, an EPR test with DMPO was employed to detect the radicals produced. As can be seen from

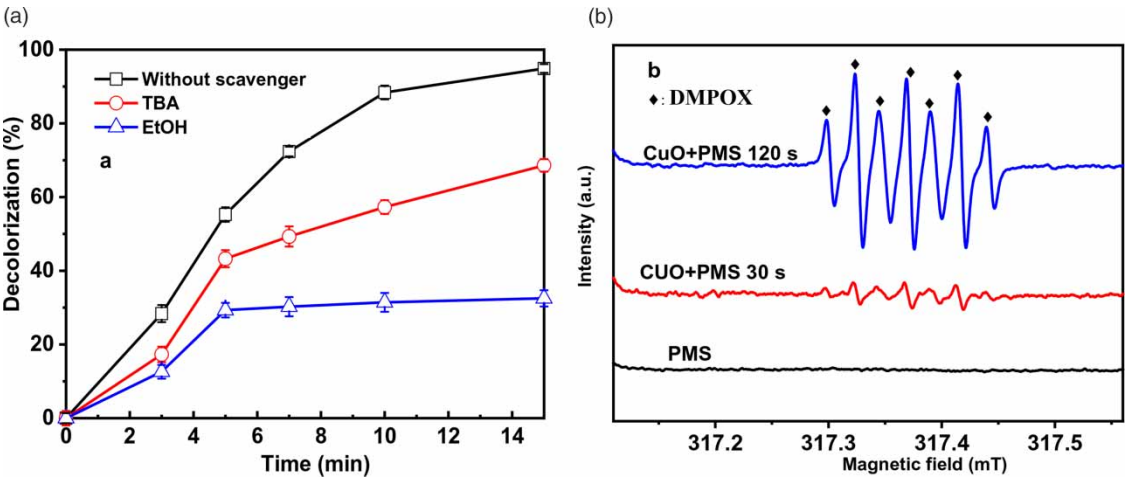

Figure 9 | (a) Effect of radical scavengers on the decolorization efficiency of AO7 in the CuO/PMS process; (b) EPR spectra obtained with the addition of DMPO. Conditions: [AO7] = 40 mg/L; [CuO] = 0.1 g/L; [PMS] = 5 mM; [DMPO] = 10 mM; room temperature.

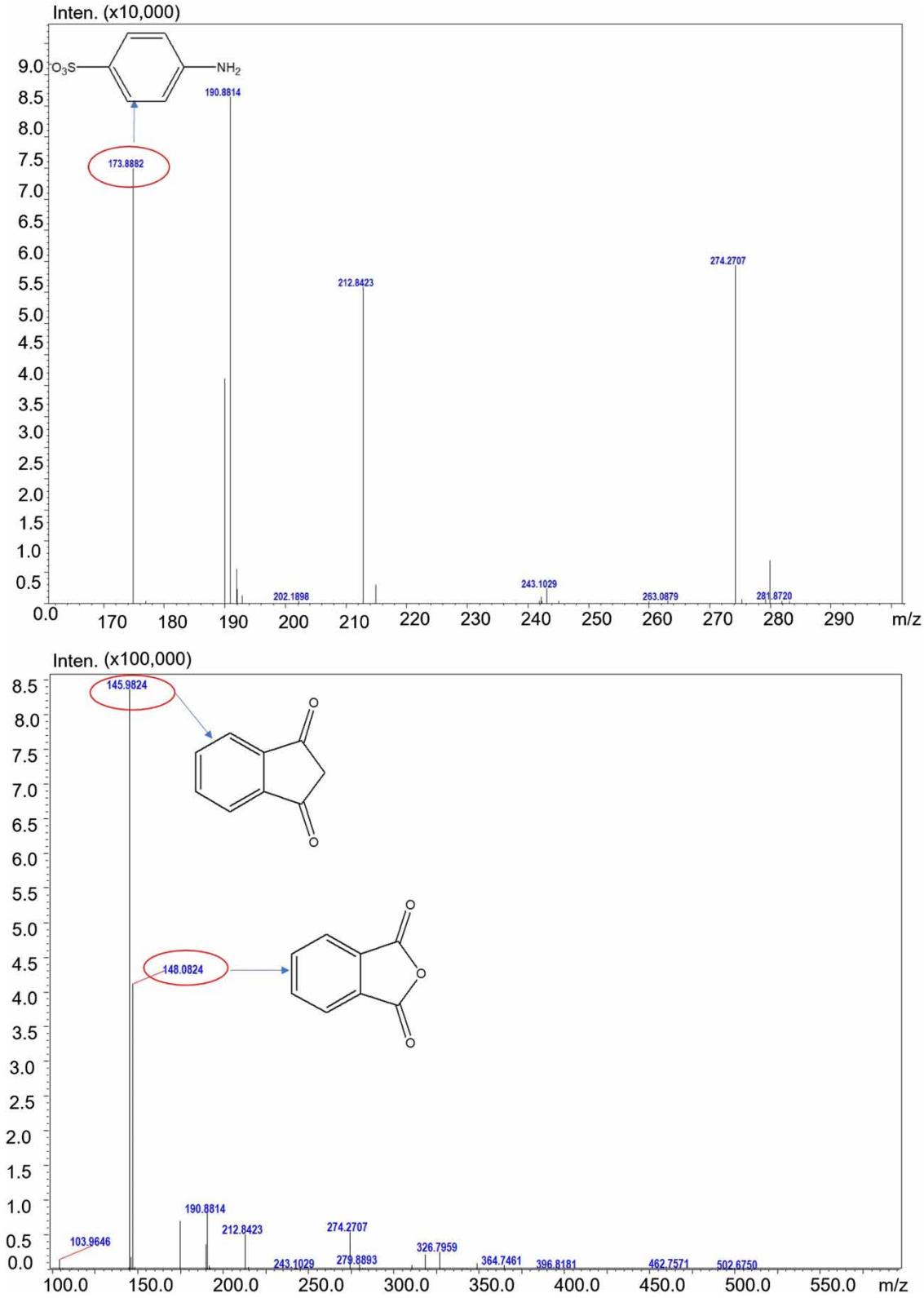

Figure 10 | The ESI IT-TOF/MS data and proposed structures of three intermediates of AO7 degradation in the CuO/PMS system.

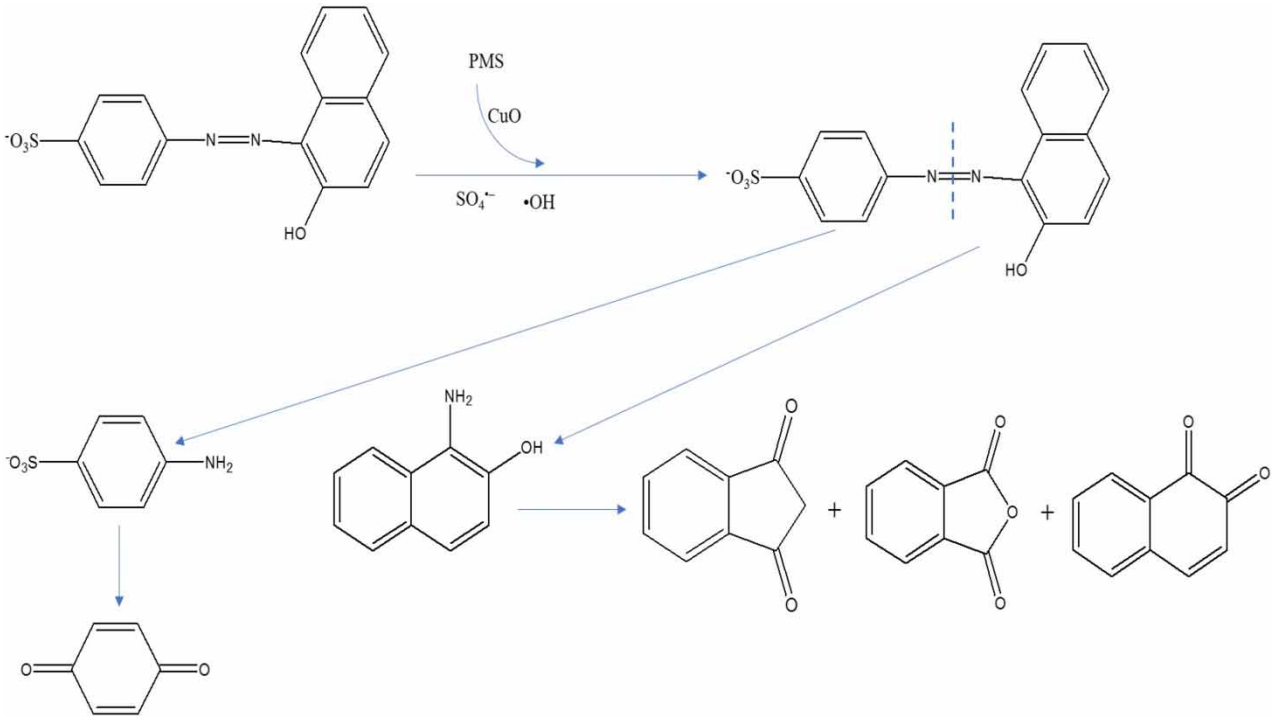

Figure 11 | Possible degradation pathways of AO7.

Figure 9(b), the characteristic peaks of DMPO-OH and DMPO-SO_4 adducts did not appear, but as the reaction proceeded, EPR signals with an intensity ratio of 1:2:1:2:1:2:1 was observed, which can be assigned to the characteristic signals of 5,5-dimethylpyrroline-(2)-oxyl-(1) (DMPOX), the nitroxide radical of DMPO. The presence of DMPOX signals can be related to the fast activation of PMS and efficient oxidation of DMPO (Li *et al.* 2017a), indicating highly effective activation of PMS in the CuO/PMS system.

TOC removal, specific oxidant efficiency and degradation pathways of AO7

TOC of AO7 solution (200 mL 40 mg/L AO7, 0.1 g/L CuO, 5 mM PMS and pH 6.65) was measured to analyze the mineralization. However, the TOC removal of AO7 was only 10.9% in the 15 min reactions, and the SOE value was 3.6. That is to say, the CuO/PMS system just led to the decomposition of AO7 molecules, while it cannot provide enough oxidation ability for the mineralization of residual organic molecules, especially with a low PMS dosage; low SOE was related to low TOC removal. The intermediates of AO7 degradation were detected by LCMS-IT-TOF (Figure 10). According to these detected intermediates and references (Lin *et al.* 2014; Shang *et al.* 2017), possible degradation pathways of AO7 are proposed in Figure 11.

CONCLUSIONS

In this study, low cost, safe and environmentally friendly CuO was synthesized through a facile one-step hydrothermal method, and then used as a PMS activator for the degradation of AO7. Radical quenchers including EtOH and TBA were used to investigate aspects of the mechanism and indicated that •OH and $SO_4^{\bullet-}$ were both involved in the decolorization of the AO7. Both •OH and $SO_4^{\bullet-}$ were suggested as the radical species in the CuO/PMS system. It was found that CuO had a high catalytic activity to degrade AO7 in the presence of PMS. Experimental results showed that AO7 decolorization efficiency was dramatically influenced by operating parameters, such as PMS concentration, CuO dosage and initial AO7 concentration. After 15 min reaction time using 5 mM PMS, a CuO dosage of

0.1 g/L, and initial pH value of 6.65, 95.38% of 40 mg/L AO7 was removed. This finding has great potential for the oxidative treatment of industrial waste and contaminated water. All the results indicated that the CuO/PMS catalytic oxidation was an efficient and clean technology for toxic and refractory industrial wastewater. Therefore, the green oxidation system consisting of CuO/PMS has great potential applications in the degradation of highly stable toxic organic pollutants.

ACKNOWLEDGEMENTS

We thank the China Postdoctoral Science Foundation (2017M620045) and Technology Innovation of Chongqing (No. cstc2015shmszx20012).

CONFLICT OF INTEREST

The authors state no conflict of interest.

REFERENCES

Ahmad, M., Teel, A. L. & Watts, R. J. 2013 Mechanism of persulfate activation by phenols. *Environmental Science & Technology* **47**, 5864–5871.

Ahmadi, M. & Ghanbari, F. 2018 Combination of UVC-LEDs and ultrasound for peroxymonosulfate activation to degrade synthetic dye: influence of promotional and inhibitory agents and application for real wastewater. *Environmental Science and Pollution Research* **25**, 6003–6014.

Anipsitakis, G. P. & Dionysiou, D. D. 2004 Radical generation by the interaction of transition metals with common oxidants. *Environmental Science & Technology* **38**, 3705–3712.

Ball, D. L. & Edwards, J. O. 1956 The kinetics and mechanism of the decomposition of caro's acid. I. *Journal of the American Chemical Society* **78**, 1125–1129.

Bandara, J., Mielczarski, J. A. & Kiwi, J. 1999 1. Molecular mechanism of surface recognition. Azo dyes degradation on Fe, Ti, and Al oxides through metal sulfonate complexes. *Langmuir* **15**, 7670–7679.

Barzegar, G., Jorfi, S., Zarezade, V., Khatebasreh, M., Mehdipour, F. & Ghanbari, F. 2018 4-Chlorophenol degradation using ultrasound/peroxymonosulfate/nanoscale zero valent iron: reusability, identification of degradation intermediates and potential application for real wastewater. *Chemosphere* **201**, 370–379.

Brillas, E. & Martínez-Huitle, C. A. 2015 Decontamination of wastewaters containing synthetic organic dyes by electrochemical methods. An updated review. *Applied Catalysis B: Environmental* **166–167**, 603–643.

Deng, J., Shao, Y., Gao, N., Deng, Y., Zhou, S. & Hu, X. 2013a Thermally activated persulfate (TAP) oxidation of antiepileptic drug carbamazepine in water. *Chemical Engineering Journal* **228**, 765–771.

Deng, J., Shao, Y., Gao, N., Xia, S., Tan, C., Zhou, S. & Hu, X. 2013b Degradation of the antiepileptic drug carbamazepine upon different UV-based advanced oxidation processes in water. *Chemical Engineering Journal* **222**, 150–158.

Deng, J., Ge, Y., Tan, C., Wang, H., Li, Q., Zhou, S. & Zhang, K. 2017 Degradation of ciprofloxacin using α-mno$_2$ activated peroxymonosulfate process: effect of water constituents, degradation intermediates and toxicity evaluation. *Chemical Engineering Journal* **330**, 1390–1400.

Ding, Y., Zhu, L., Wang, N. & Tang, H. 2013 Sulfate radicals induced degradation of tetrabromobisphenol A with nanoscaled magnetic $CuFe_2O_4$ as a heterogeneous catalyst of peroxymonosulfate. *Applied Catalysis B: Environmental* **129**, 153–162.

Du, X., Zhang, Y., Hussain, I., Huang, S. & Huang, W. 2017 Insight into reactive oxygen species in persulfate activation with copper oxide: activated persulfate and trace radicals. *Chemical Engineering Journal* **313**, 1023–1032.

Duan, X., Ao, Z., Sun, H., Indrawirawan, S., Wang, Y., Kang, J., Liang, F., Zhu, Z. H. & Wang, S. 2015 Nitrogen-doped graphene for generation and evolution of reactive radicals by metal-free catalysis. *ACS Applied Materials & Interfaces* **7**, 4169–4178.

Guan, Y.-H., Ma, J., Ren, Y.-M., Liu, Y.-L., Xiao, J.-Y., Lin, L.-Q. & Zhang, C. 2013 Efficient degradation of atrazine by magnetic porous copper ferrite catalyzed peroxymonosulfate oxidation via the formation of hydroxyl and sulfate radicals. *Water Research* **47**, 5431–5438.

Hu, P. & Long, M. 2016 Cobalt-catalyzed sulfate radical-based advanced oxidation: a review on heterogeneous catalysts and applications. *Applied Catalysis B: Environmental* **181**, 103–117.

Hu, J., Dong, H., Qu, J. & Qiang, Z. 2017 Enhanced degradation of iopamidol by peroxymonosulfate catalyzed by two pipe corrosion products (CuO and δ-mno2). *Water Research* **112**, 1–8.

Jaafarzadeh, N., Ghanbari, F. & Alvandi, M. 2017 Integration of coagulation and electro-activated HSO_5^- to treat pulp and paper wastewater. *Sustainable Environment Research* **27**, 223–229.

Jiang, B., Liu, Y., Zheng, J., Tan, M., Wang, Z. & Wu, M. 2015 Synergetic transformations of multiple pollutants driven by Cr(VI)–sulfite reactions. *Environmental Science & Technology* **49**, 12363–12371.

Lee, H., Lee, H.-J., Jeong, J., Lee, J., Park, N.-B. & Lee, C. 2015 Activation of persulfates by carbon nanotubes: oxidation of

organic compounds by nonradical mechanism. *Chemical Engineering Journal* **266**, 28–33.

Lei, Y., Chen, C.-S., Tu, Y.-J., Huang, Y.-H. & Zhang, H. 2015 Heterogeneous degradation of organic pollutants by persulfate activated by CuO-Fe_3O_4: mechanism, stability, and effects of pH and bicarbonate ions. *Environmental Science & Technology* **49**, 6838–6845.

Li, H., Li, Y., Xiang, L., Huang, Q., Qiu, J., Zhang, H., Sivaiah, M. V., Baron, F., Barrault, J., Petit, S. & Valange, S. 2015 Heterogeneous photo-Fenton decolorization of Orange II over Al-pillared Fe-smectite: response surface approach, degradation pathway, and toxicity evaluation. *Journal of Hazardous Materials* **287**, 32–41.

Li, J., Lin, H., Zhu, K. & Zhang, H. 2017a Degradation of Acid Orange 7 using peroxymonosulfate catalyzed by granulated activated carbon and enhanced by electrolysis. *Chemosphere* **188**, 139–147.

Li, J., Ye, P., Fang, J., Wang, M., Wu, D., Xu, A. & Li, X. 2017b Peroxymonosulfate activation and pollutants degradation over highly dispersed CuO in manganese oxide octahedral molecular sieve. *Applied Surface Science* **422**, 754–762.

Liang, H.-Y., Zhang, Y.-Q., Huang, S.-B. & Hussain, I. 2013 Oxidative degradation of p-chloroaniline by copper oxidate activated persulfate. *Chemical Engineering Journal* **218**, 384–391.

Lin, H., Zhang, H. & Hou, L. 2014 Degradation of C. I. Acid Orange 7 in aqueous solution by a novel electro/Fe_3O_4/PDS process. *Journal of Hazardous Materials* **276**, 182–191.

Liu, Y., He, X., Duan, X., Fu, Y., Fatta-Kassinos, D. & Dionysiou, D. D. 2016 Significant role of UV and carbonate radical on the degradation of oxytetracycline in UV-AOPs: kinetics and mechanism. *Water Research* **95**, 195–204.

López-López, A., Pic, J. S. & Debellefontaine, H. 2007 Ozonation of azo dye in a semi-batch reactor: a determination of the molecular and radical contributions. *Chemosphere* **66**, 2120–2126.

Luo, X., Liang, H., Qu, F., Ding, A., Cheng, X., Tang, C. Y. & Li, G. 2018 Free-standing hierarchical α-MnO_2@CuO membrane for catalytic filtration degradation of organic pollutants. *Chemosphere* **200**, 237–247.

Neta, P., Huie, R. E. & Ross, A. B. 1988 Rate constants for reactions of inorganic radicals in aqueous-solution. *Journal of Physical and Chemical Reference Data* **17**, 1027–1284.

Oh, W.-D., Dong, Z. & Lim, T.-T. 2016 Generation of sulfate radical through heterogeneous catalysis for organic contaminants removal: current development, challenges and prospects. *Applied Catalysis B: Environmental* **194**, 169–201.

Qi, C., Liu, X., Zhao, W., Lin, C., Ma, J., Shi, W., Sun, Q. & Xiao, H. 2015 Degradation and dechlorination of pentachlorophenol by microwave-activated persulfate. *Environmental Science and Pollution Research* **22**, 4670–4679.

Rao, M. P., Sathishkumar, P., Mangalaraja, R. V., Asiri, A. M., Sivashanmugam, P. & Anandan, S. 2018 Simple and low-cost synthesis of CuO nanosheets for visible-light-driven photocatalytic degradation of textile dyes. *Journal of Environmental Chemical Engineering* **6**, 2003–2010.

Shang, K., Wang, X., Li, J., Wang, H., Lu, N., Jiang, N. & Wu, Y. 2017 Synergetic degradation of Acid Orange 7 (AO7) dye by DBD plasma and persulfate. *Chemical Engineering Journal* **311**, 378–384.

Yang, S., Wang, P., Yang, X., Shan, L., Zhang, W., Shao, X. & Niu, R. 2010 Degradation efficiencies of azo dye Acid Orange 7 by the interaction of heat, UV and anions with common oxidants: persulfate, peroxymonosulfate and hydrogen peroxide. *Journal of Hazardous Materials* **179**, 552–558.

Zhang, T., Zhu, H. & Croué, J.-P. 2013 Production of sulfate radical from peroxymonosulfate induced by a magnetically separable $CuFe_2O_4$ spinel in water: efficiency, stability, and mechanism. *Environmental Science & Technology* **47**, 2784–2791.

Zhang, T., Chen, Y., Wang, Y., Le Roux, J., Yang, Y. & Croué, J.-P. 2014 Efficient peroxydisulfate activation process not relying on sulfate radical generation for water pollutant degradation. *Environmental Science & Technology* **48**, 5868–5875.

First received 16 July 2018; accepted in revised form 1 October 2018. Available online 2 November 2018